Development of H^- conductive oxyhydrides

Efficiency of the hydrogen transport in solids is a key to determining the performance of electrochemical devices such as fuel cells and batteries. Indeed, active studies on proton (H^+) conduction in oxides and other systems have been carried out. In contrast, hydrogen can also accept one electron to form a hydride ion (H^-). Hydride ions are also attractive for use as charge carriers because they are similar in size to oxide and fluoride ions, which are suitable for fast ionic conduction, while they also exhibit strong reducing properties owing to their standard H^-/H_2 redox potential (–2.3 V), which is comparable to that of Mg/Mg^{2+} (–2.4 V). Hydride ion conductors may therefore be applied in energy storage/conversion devices with high energy densities. However, pure H^- conduction has been verified only for a few hydrides of alkaline earth metals such as BaH_2 [1]. Unfortunately, utilization of the hydrides is difficult because of their structural inflexibility, which makes it difficult to control the lattice structure to create smooth transport pathways as well as the conducting hydride ion content. We have considered oxyhydrides, where hydride ions and oxide ions share anion sublattices, as candidate hydride conductors equipped with flexible anion sublattices.

A further complication in achieving pure H^- conduction in an oxide framework structure is the difficulty in inhibiting electron conduction. It is well known that hydride ions act as electron donors in oxides, transferring electrons from hydride ions to the lattice. This causes the conduction of electrons accompanied by a characteristic change in the hydrogen charge from H^- to H^+. Indeed, the perovskite and mayenite-type oxyhydrides are dominated by electron conduction caused by the dissociation of hydride ions into electrons and protons [2,3]. In the present study, we attempted to synthesize a series of K_2NiF_4-type oxyhydrides, $La_{2-x-y}Sr_{x+y}LiH_{1-x+y}O_{3-y}$ ($0 \le x \le 1$, $0 \le y \le 2$, $0 \le x+y \le 2$), which are equipped with cation sublattices featuring cations more electron-donating than H^- and anion sublattices that exhibit flexibility in the storage of H^-, O^{2-}, and vacancies [4].

The oxyhydrides $La_{2-x-y}Sr_{x+y}LiH_{1-x+y}O_{3-y}$ were synthesized by a solid-state reaction under high pressure and temperature using a cubic anvil cell. Synchrotron X-ray diffraction (SXRD) measurements in this study were performed at SPring-8 **BL02B2**. A Debye-Scherrer diffraction camera was used for measurements at 298 K. The SXRD pattern of La_2LiHO_3 ($x=y=0$) was assigned to the K_2NiF_4-type structure with an orthorhombic *Immm* symmetry. Figure 1 shows SXRD patterns of solid solutions between La_2LiHO_3 and Sr_2LiH_3O, represented as $La_{2-y}Sr_yLiH_{1+y}O_{3-y}$ ($x=0$, $0 \le y \le 2$). Here, the H:O ratio changes accordingly as La is substituted with Sr, maintaining the simple A_2BX_4 composition (*A*:La, Sr; *B*:Li; *X*:O, H). In $La_{2-x}Sr_xLiH_{1-x}O_3$ ($0 \le x \le 1$, $y = 0$) and

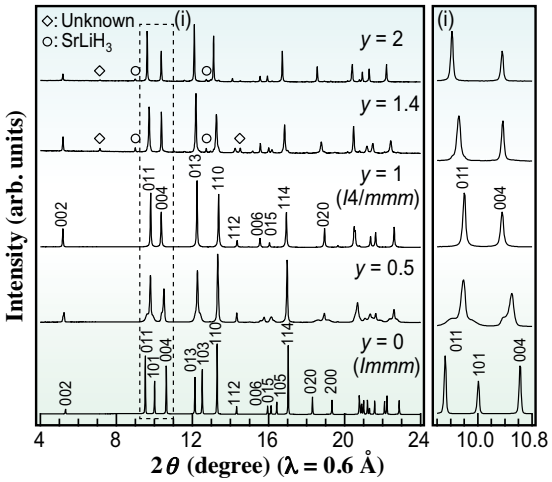

Fig. 1. Comparison of the synchrotron X-ray diffraction patterns for $La_{2-x-y}Sr_{x+y}LiH_{1-x+y}O_{3-y}$ ($x = 0$, $0 \le y \le 2$).

$La_{1-x}Sr_{1+x}LiH_{2-x}O_2$ ($0 \le x \le 1$, $y = 1$), Regarding the Sr-substituted series of $La_{2-y}Sr_yLiH_{1+y}O_{3-y}$, the diffraction peaks continuously shifted to lower angles with increasing *y* and the lattice symmetry changed from *Immm* ($y < 1$) to *I*4/*mmm* ($y \ge 1$).

The compositions and structures of $La_{2-y}Sr_yLiH_{1+y}O_{3-y}$ ($y = 0, 1, 2$) were determined by X-ray and neutron Rietveld analyses. Figure 2 shows the determined crystal structures of $La_{2-y}Sr_yLiH_{1+y}O_{3-y}$. In La_2LiHO_3, the two apical sites of the LiX_6 octahedra are occupied only by O^{2-}, while the four in-plane apexes are orderly occupied by O^{2-} and H^- in an orderly manner. These results indicate that the highly charged cations, i.e., La^{3+} and Sr^{2+}, require highly charged anions around them. $LaSrLiH_2O_2$ is composed of tetragonal $(LiH_2)^-$ and $(LaSrO_2)^+$ layers alternately stacked along the *c* axis. A further increase in the hydride content up to Sr_2LiH_3O results in the formation of $(Sr_2HO)^+$ layers. A Rietveld analysis for the anion deficient series, $La_{1-x}Sr_{1+x}LiH_{2-x}O_2$ ($x > 0$, $y = 1$), was also carried out. As a result, it was clarified that vacancies were introduced at the LiH_4 plane with increasing *x*.

The ionic conductivities of $La_{2-x-y}Sr_{x+y}LiH_{1-x+y}O_{3-y}$ were examined by impedance measurement. For the vacancy-free composition $La_{2-y}Sr_yLiH_{1+y}O_{3-y}$ ($x = 0$), the conductivity increases with increasing H^- content, with the highest conductivity of 3.2×10^{-5} S cm^{-1} at 573 K being observed for Sr_2LiH_3O ($y = 2$). The introduction of hydride ions into the anion sites of the K_2NiF_4 structure improved the ionic conductivity, suggesting that the primary charge carriers are these hydride ions. The conduction is further facilitated by the introduction of vacancies, as can be seen for both $La_{2-x}Sr_xLiH_{1-x}O_3$ ($y = 0$) and $La_{1-x}Sr_{1+x}LiH_{2-x}O_2$ ($y = 1$), reaching 2.1×10^{-4} S cm^{-1} for $La_{0.6}Sr_{1.4}LiH_{1.6}O_2$ at 590 K.

To further identify the nature of charge carriers, an all-

solid-state Ti/La_2LiHO_3/TiH_2 cell was constructed using La_2LiHO_3 as the solid electrolyte, and the galvanostatic discharge reaction was examined. Figure 3(a) shows the discharge curve of the cell, displaying a constant discharge current of 0.5 μA at 573 K. The cell showed an initial open circuit voltage of 0.28 V, which is consistent with the theoretical value calculated from the standard Gibbs energy of formation of TiH_2. During the electrochemical reaction, the cell voltage dropped rapidly from 0.28 V to 0.06 V, and then decreased gradually to 0.0 V. This steep drop-off in the first reaction step corresponds to an increase in the hydride ion content at the anode in accordance with the constant current discharge reaction

$$Ti + xH^- \rightarrow TiH_x + xe^- ,$$

where the reaction at the cathode is as follows:

$$TiH_2 + xe^- \rightarrow TiH_{2-x} + xH^- .$$

These discharge reactions were confirmed by observation of the phases that appeared following the reaction. Figure 3(b) shows the synchrotron X-ray diffraction patterns for the cathode, electrolyte, and anode, both before and after the reaction. The absence of any variation in the diffraction patterns of the electrolyte indicates that the La_2LiHO_3 electrolyte is stable when in contact with the Ti and TiH_2 electrodes during the reaction. The phase changes detected for the cathode and anode materials are consistent with those expected from the Ti-H phase diagram [5], where the δ-TiH_2 phase releases hydrogen and is transformed into α-Ti through a two-phase (α-TiH_b + δ-TiH_{2-a}) coexistence region. In the case of the cathode, additional diffraction peaks corresponding to the α-Ti phase were detected. In addition, the signals corresponded to a shift of TiH_2 to a higher angle, thus indicating that lattice shrinkage takes place with the release of hydrogen from TiH_2. In the case of the anode, peaks corresponding to the δ-TiH_2 phase were detected. These results indicate that during the electrochemical reaction, hydride ions are released from the TiH_2 cathode and diffuse into the Ti anode through the La_2LiHO_3.

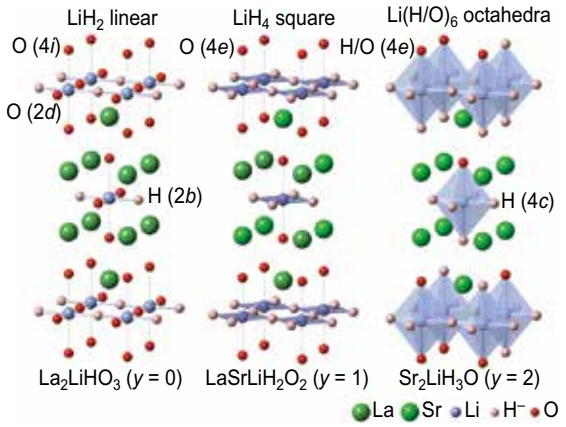

Fig. 2. Crystal structures of $La_{2-x-y}Sr_{x+y}LiH_{1-x+y}O_{3-y}$ ($x = 0$, $y = 0, 1, 2$).

In conclusion, pure H^- conduction was realized in the $La_{2-x-y}Sr_{x+y}LiH_{1-x+y}O_{3-y}$ system. The present successful construction of an all-solid-state electrochemical cell exhibiting H^- diffusion confirms not only the capability of the oxyhydride to act as H^- solid electrolyte but also the possibility of developing electrochemical solid devices based on H^- conduction.

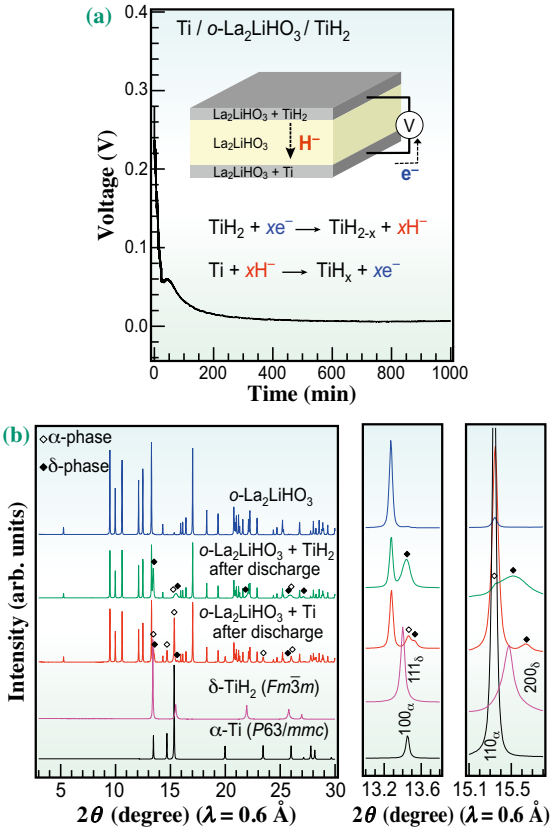

Fig. 3. All-solid-state hydride cell. **(a)** Discharge curve for a solid-state battery with the Ti/La_2LiHO_3/TiH_2 structure. The inset shows an illustration of the cell and the proposed electrochemical reaction. **(b)** X-ray diffraction patterns for the electrolyte (La_2LiHO_3), cathode (TiH_2 + La_2LiHO_3), and anode (Ti + La_2LiHO_3) materials after the reaction.

Genki Kobayashi[a,*] and Ryoji Kanno[b]

[a] Research Center of Integrative Molecular Science, Institute for Molecular Science
[b] School of Materials and Chemical Technology, Tokyo Institute of Technology

*Email: gkobayashi@ims.ac.jp

References

[1] M.C. Verbraeken *et al.*: Nat. Mater. **14** (2015) 95.
[2] K. Hayashi *et al.*: Nature **419** (2003) 462.
[3] Y Kobayashi *et al.*: Nat. Mater. **11** (2012) 507.
[4] *G. Kobayashi, Y. Hinuma, S. Matsuoka, A. Watanabe, M. Iqbal, M. Hirayama, M. Yonemura, T. Kamiyama, I. Tanaka R. Kanno: Science **351** (2016) 1314.*
[5] A. San-Martin, F.D. Manchester: Bulletin of Alloy Phase Diagrams **8** (1987) 30.